Supplementary Material

Supplemental Methods:

Histological analysis

Liver samples were fixed in 4% paraformaldehyde overnight or immediately embedded in Tissue-Tek OCT compound. Formalin-fixed piece was embedded by paraffin and sectioned at 5 μm for hematoxylin and eosin (H&E) staining, Picrosirius red staining and immunohistochemistry (F4/80). Oil Red O staining and DHE staining were performed with the OCT-embedded and frozen tissue sections. Quantification analysis was performed by Image J software.

Measurements of plasma and liver parameters

The blood samples were collected in a tube containing 3.2% buffered sodium citrate and then centrifugated at 1,500×g for 20 min to obtain plasma. Plasma FVII levels were quantified by a FVII ELISA kit (Cloud-Clone Corp, China) according to the manufacturer's instructions. Plasma alanine aminotransferase (ALT) and aspartate aminotransferase (AST) were measured by commercial kits (ShenSuo UNF, Shanghai, China) following the manufacturer's instructions. TG and TC levels from the liver were measured by commercial kits (Cat# E1013 for TG, Cat# E1015 for TC; Applygen, Beijing, China), and liver NEFA were measured by another kit (Cat# A042-2-1; Jiancheng, Jiangsu, China).

Plasmids construction

ShRNA targeting F7 mRNA was designed by the BLOCK-iT RNAi Designer (ThermoFisher, Waltham, MA, USA). Oligonucleotides were annealed and then cloned into the BLOCK-iT™ U6 RNAi Entry Vector (ThermoFisher, Waltham, MA, USA; cat#K494500), followed by homologous recombination into the pAd/BLOCK-iT™-DEST RNAi Gateway® adenovirus Vector (ThermoFisher, Waltham, MA, USA; cat#V49220). The U6 promoter was used in this construct. As a control, we utilized shRNA targeting LacZ (CTACACAAATCAGCGATTT). F7-flag expression plasmids were generated by standard PCR based procedures and cloned into the pLVX expression lentivirus vector (Clontech, Mountain View, CA, USA) or pENTR™ Directional TOPO® Cloning vector (ThermoFisher, Waltham, MA, USA; cat#240020). The later vector was then recombined into the pAd/CMV/V5-DEST™ Gateway™ Adenoviral Expression vector (ThermoFisher, Waltham, MA, USA; cat#V4932). T7 promoter was utilized in adenoviral system to enhance F7 expression. As a control, an adenoviral vector expressing LacZ (Ad-ctrl) was prepared. The F7 mutant plasmid with signal peptide deletion (ΔAA 2-24) was subcloned from pLVX-F7-flag by the NEBuilder HiFi DNA assembly kit (NEB, Ipswich, MA, USA). The primers were listed in Table S1.

Adenovirus production

The recombinant adenovirus plasmids were linearized with PacI restriction enzyme and

transfected into HEK293A cells (ThermoFisher, Waltham, MA, USA) to generate adenovirus. The adenovirus was purified by cesium chloride ultracentrifugation. The viral titers were quantified by cytopathic effect assay.

Coagulation homeostasis analysis

The mice were anesthetized with isoflurane, and their tails were cut by 5 mm. The tails were then placed into a beaker containing 37°C physiological saline solution and the bleeding time was recorded when the bleeding from the tails stopped. For the clotting time test, blood samples were collected from the retro-orbital sinus vein into a capillary blood collection tube without anti-coagulant. At 30-second intervals, the tubes were tilted to observe the blood's flow ability. The clotting time was recorded when the blood clotting occurred. For coagulation four indices, blood samples were collected in a tube containing 3.2% buffered sodium citrate and then centrifugated at 3,500×g for 10 min to obtain plasma. The plasma was then put into Sysmex CS-2400 automated coagulation analyzer (Sysmex, Kobe, Japan) to measure coagulation four indices: prothrombin time (PT), activated partial thromboplastin time (APTT), thrombin time (TT) and plasma fibrinogen (FIB) levels.

$FeCl_3$ induced thrombosis model

The mice were anesthetized with pelltobarbitalum natricum, and then the right common carotid arteries were carefully exposed and separated from surrounded tissue. To record blood flow, a doppler flow probe (Transonic Systems, New York, USA) was placed on

the carotid artery. When a 2-mm piece of filter paper saturated with 30% $FeCl_3$ (Sigma-Aldrich, Burlington, MA, USA) was wrapped on the surface of carotid artery, the blood flow was immediately monitored. 3 minutes later, the filter paper was removed, and the occlusion time was defined when blood flow < 0.05 mL/min.

Cellular lipid assay

Hepatocytes were treated with 1 mM mixed free fatty acids (FFA) consisting of palmitic acid (PA) and oleic acid (OA) at a ratio of 1:2 for 24 h to induce cellular lipid accumulation. Then cells were fixed with 4% paraformaldehyde and stained with Nile red (Sigma-Aldrich, Burlington, MA, USA) for 15 min or Oil Red O (Sigma-Aldrich, Burlington, MA, USA) for 1 h to examine lipid droplets. Intracellular TG contents were assessed as above described.

Tissue and cellular lipotoxicity assay

Frozen liver sections and primary hepatocytes were washed with PBS twice and then stained with 10 μM DHE (ThermoFisher, Waltham, MA, USA) for 30 min to detect superoxide anion radical. For mitochondrial function analysis, hepatocytes were incubated with 500 nM Mito-Tracker Red (ThermoFisher, Waltham, MA, USA) for 30 min to detect mitochondrial content and 10 mM JC-1 (Yeasen Biotech, Shanghai, China) for 30 min to detect mitochondrial membrane potential. The staining cells were imaged by a fluorescence microscope and analyzed by Image J software.

Immunofluorescence

Primary hepatocytes were fixed with 4% formalin for 15 min, then permeabilized with 0.2% Triton X-100 and blocked with 5% BSA for 1 h. The paraffin sections were subjected to deparaffinized and antigen repair, and then blocked with 5% BSA (37°C, 1 h). Subsequently, they were incubated with the appropriate primary antibodies overnight and then treated with the corresponding secondary antibodies for 1 h. The nuclei of cells were counterstained using DAPI for 10 min prior to mounting on a slide and imaging via two-photon microscope (Olympus, USA).

Immunoblot

Liver tissues and hepatocytes were lysed with lysis buffer (50 mM Tris-HCl, 150 mM NaCl, 1% SDS, pH 8.0) containing protease inhibitors and phosphorylation inhibitors (ThermoFisher, Waltham, MA, USA). Then the protein was separated by a 10% SDS-PAGE gel and transferred onto a polyvinylidene difluoride membrane (Millipore, Billerica, MA, USA). Membranes were blocked with 5% BSA and incubated with specific primary antibodies overnight, followed by incubation with the secondary antibodies (1:50,000; Jackson Immuno Research Laboratory, West Grove, PA, USA) for 1 h at room temperature. Immunoreactivities were detected with enhanced chemiluminescent autoradiography (Millipore, Billerica, MA, USA). Antibodies against FVII (Cat# 197656), p-mTOR (Cat# 109268), and mTOR (Cat# ab32028) were purchased from Abcam (Cambridge, UK). Antibodies against p-AKT (Ser 473) (Cat# 9271), AKT(Cat# 4691), p-ERK1/2(Cat# 4377), ERK(Cat# 4695), p-p38MAPK(Cat#

4511), p38MAPK(Cat# 8690), HNF4α(Cat# 3113), p-IR (Cat# 3024), total IR(Cat# 3020), IRS1(Cat# 2382), PDK1(Cat# 5662), PTEN(Cat# 9188), PP2A-A (Cat# 2041) and β-Actin (Cat# 4967) were purchased from Cell Signaling Technology (CST, MA, USA). Antibody against CD36 (Cat# NB400-144) was purchased from Novus Biologicals (Littleton, CO, USA). Antibody against PTP1B (Cat# 11334-1-AP) was purchased from Proteintech (Hubei, China). Antibody against IRS2 (Cat# A7945) was purchase from Abclonal (Hubei, China).

Real-time PCR

Total RNA was isolated from hepatocytes or liver tissues using the TRIzol reagent (ThermoFisher, Waltham, MA, USA) following manufacturer's instruction. RNA was reverse transcribed to cDNA using a First Strand cDNA Synthesis Kit (Vazyme Biotech, Nanjing, China). Real-time quantitative PCR (RT-qPCR) was performed in a LightCycler® 480 Multiwell Plate 384 PCR system (Roche) using SYBR Green Supermix (Vazyme Biotech, Nanjing, China) and normalized to the expression of 18S. The primer sequences used for RT-qPCR was available in Table S1.

Supplemental Figures

Figure S1

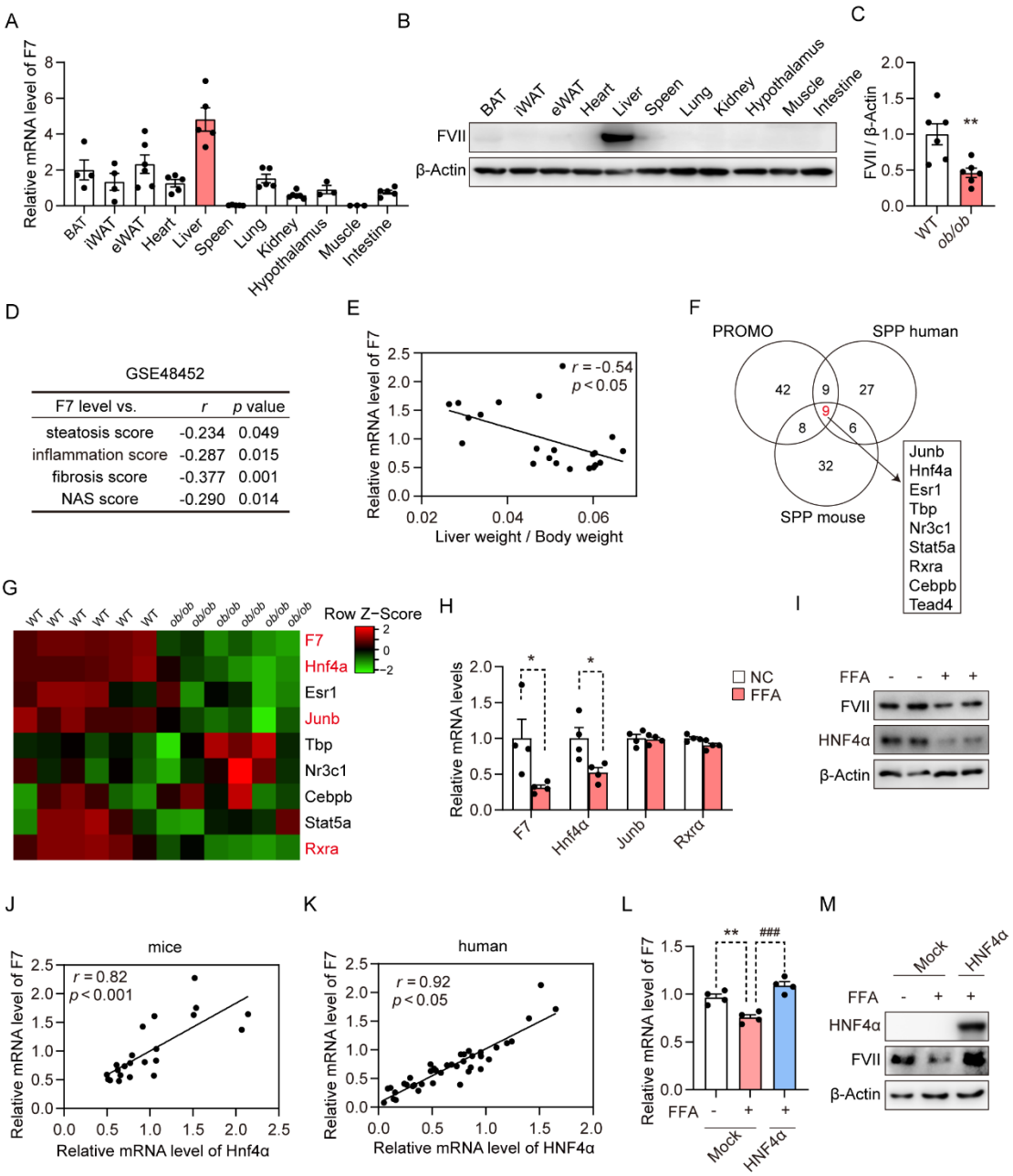

Figure S1. FVII is downregulated by HNF4α during NAFLD, related to Figure 1

(A) RT-qPCR analysis of *F7* mRNA level in the indicated tissues from 8-week-old male C57BL/6J mice (n = 4-5).

(B) Immunoblot analysis of FVII protein level in the indicated tissues from C57BL/6J mice. β-Actin was used as a loading control.

(C) Quantitative analysis of FVII protein level from panel (G) in Figure1.

(D) Correlation analysis between hepatic *F7* mRNA level and NAFLD score from GSE48452 (n = 71).

(E) Correlation analysis between hepatic *F7* mRNA level and liver to body weight ratio in C57BL/6J mice fed *ad libitum* with HFD for 24 weeks.

(F) Venn diagram of candidate transcription factors of F7 predicated by PROMO (human F7) and SPP (human and murine F7).

(G) Heatmap of relative expression of candidate transcription factors in the livers of WT and *ob/ob* mice (GSE49195).

(H, I) RT-qPCR analysis (H) and immunoblots analysis (I) of FVII and HNF4α in L02 cells treated with FFAs for 24 h.

(J, K) Correlation analysis between hepatic *F7* mRNA level and *Hnf4α* mRNA level in mice (J, n = 22) and human (K, n = 45).

(L, M) RT-qPCR analysis (L) and immunoblots analysis (M) of FVII expression in L02 cells transfected with mock or HNF4α vector in the present or absent of FFAs.

Data are presented as mean ± S.E.M. Significance was assessed by Student's t test (C, H), Pearson correlation (E, K), Spearman correlation (D, J), or one-way ANOVA (L). * $P < 0.05$, ** $P < 0.01$, *** or $^{###}$ $P < 0.001$ versus control.

Figure S2

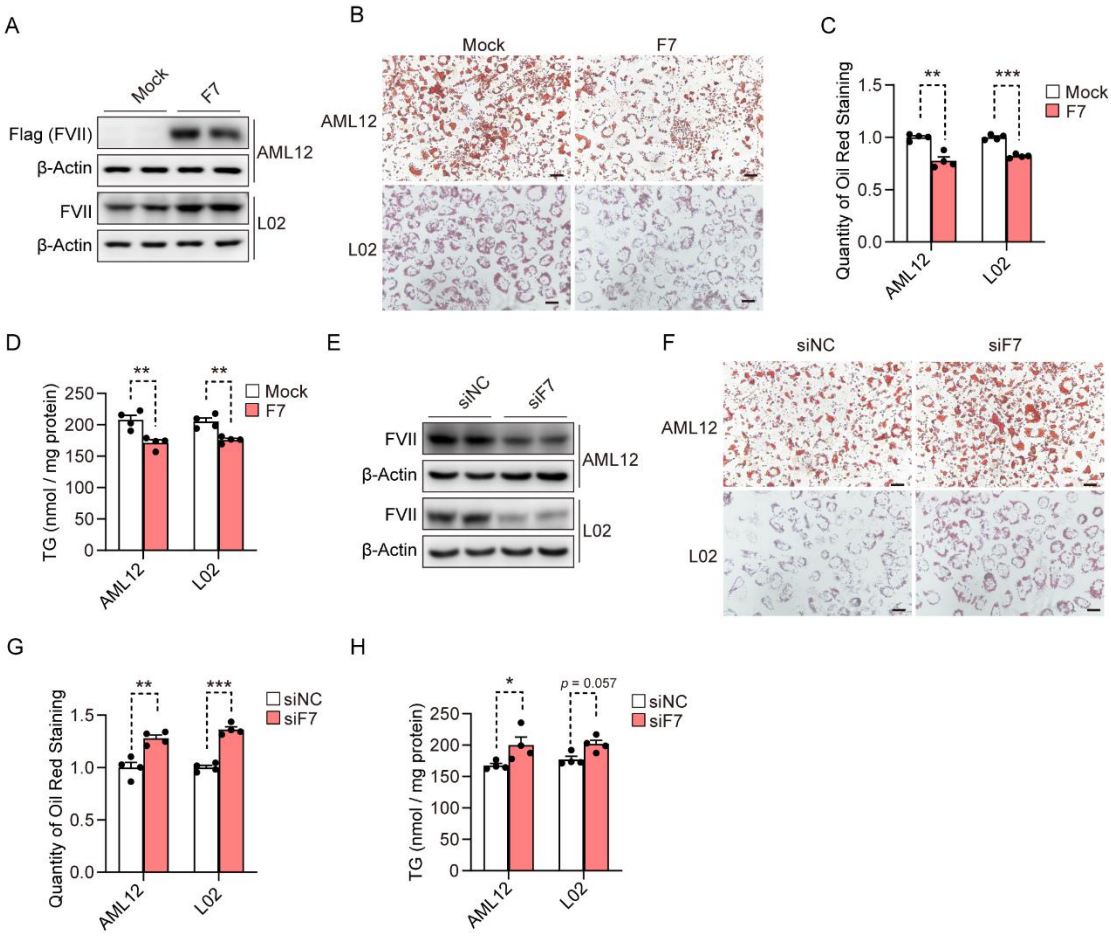

Figure S2. FVII impairs FFA-induced lipid accumulation in hepatocytes, related to Figure 2

(A) Immunoblot analysis of FVII protein levels in F7-overexpressed AML12 and L02 cells. β-Actin was used as a loading control.

(B) Representative images of Oil Red O staining of F7-overexpressed AML12 and L02 cells. Scale bar, 100 μm.

(C) Quantification of Oil Red O staining from panel (B).

(D) Cellular TG contents in F7-overexpressed AML12 and L02 cells.

(E) Immunoblot analysis of FVII protein levels in F7-silenced AML12 and L02 cells. β-Actin was used as a loading control.

(F) Representative images of Oil Red O staining of in F7-silenced AML12 and L02 cells. Scale bar, 100 μm.

(G) Quantification of Oil Red O staining from panel (F).

(H) Cellular TG contents in F7-silenced AML12 and L02 cells.

Data are presented as mean ± S.E.M. Significance was assessed by Student's *t* test (C, D, G, H) or Mann-Whitney *U* test (H). * $P < 0.05$, ** $P < 0.01$, *** $P < 0.001$ versus control.

Figure S3

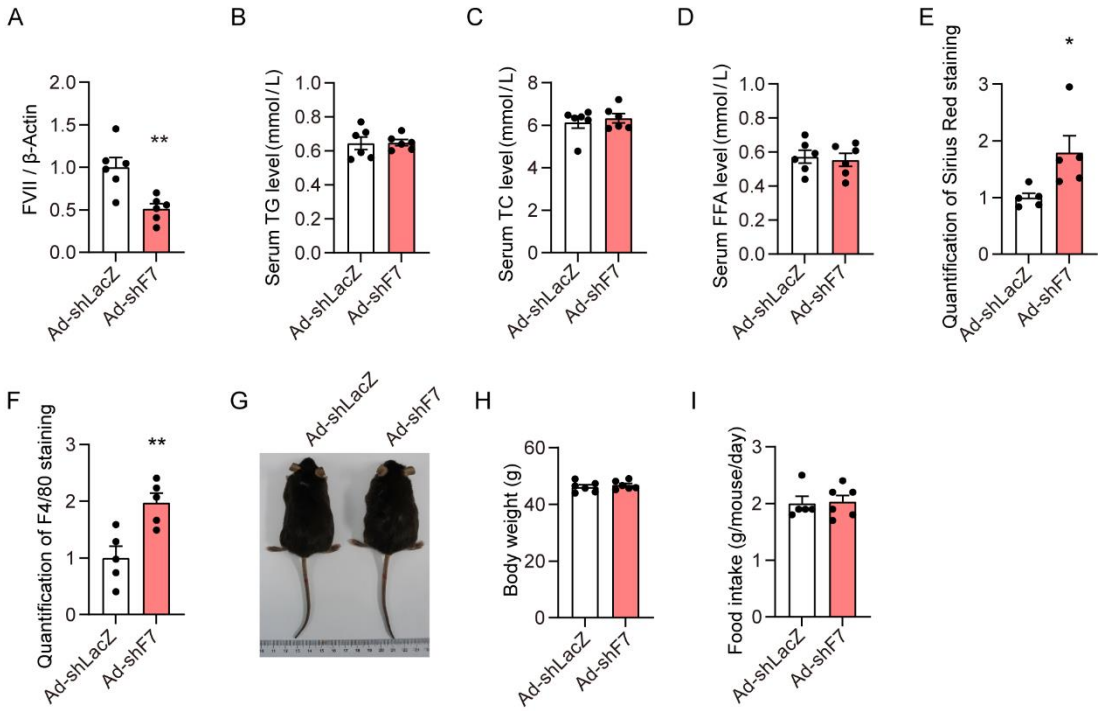

Figure S3. Evaluation of the metabolic parameters in hepatic F7 knockdown mice, related to Figure 2

(A) Quantitative analysis of FVII expression from panel (H) in Figure 2.

(B) Serum TG levels of Ad-shLacZ and Ad-shF7 DIO mice (n = 6 / group).

(C) Serum TC levels of Ad-shLacZ and Ad-shF7 DIO mice (n = 6 / group).

(D) Serum FFA levels of Ad-shLacZ and Ad-shF7 DIO mice (n = 6 / group).

(E) Quantitative analysis of Sirius Red staining from panel (O) in Figure 2.

(F) Quantitative analysis of F4/80 staining from panel (O) in Figure 2.

(G) The representative photograph of Ad-shLacZ and Ad-shF7 DIO mice.

(H) Body weight of Ad-shLacZ and Ad-shF7 DIO mice (n = 6 / group).

(I) Food intake of Ad-shLacZ and Ad-shF7 DIO mice (n = 6 / group).

Data are presented as mean ± S.E.M. Significance was assessed by Student's t test (A-

F, H) or Mann-Whitney *U* test (I). * $P < 0.05$, ** $P < 0.01$ versus control.

Figure S4

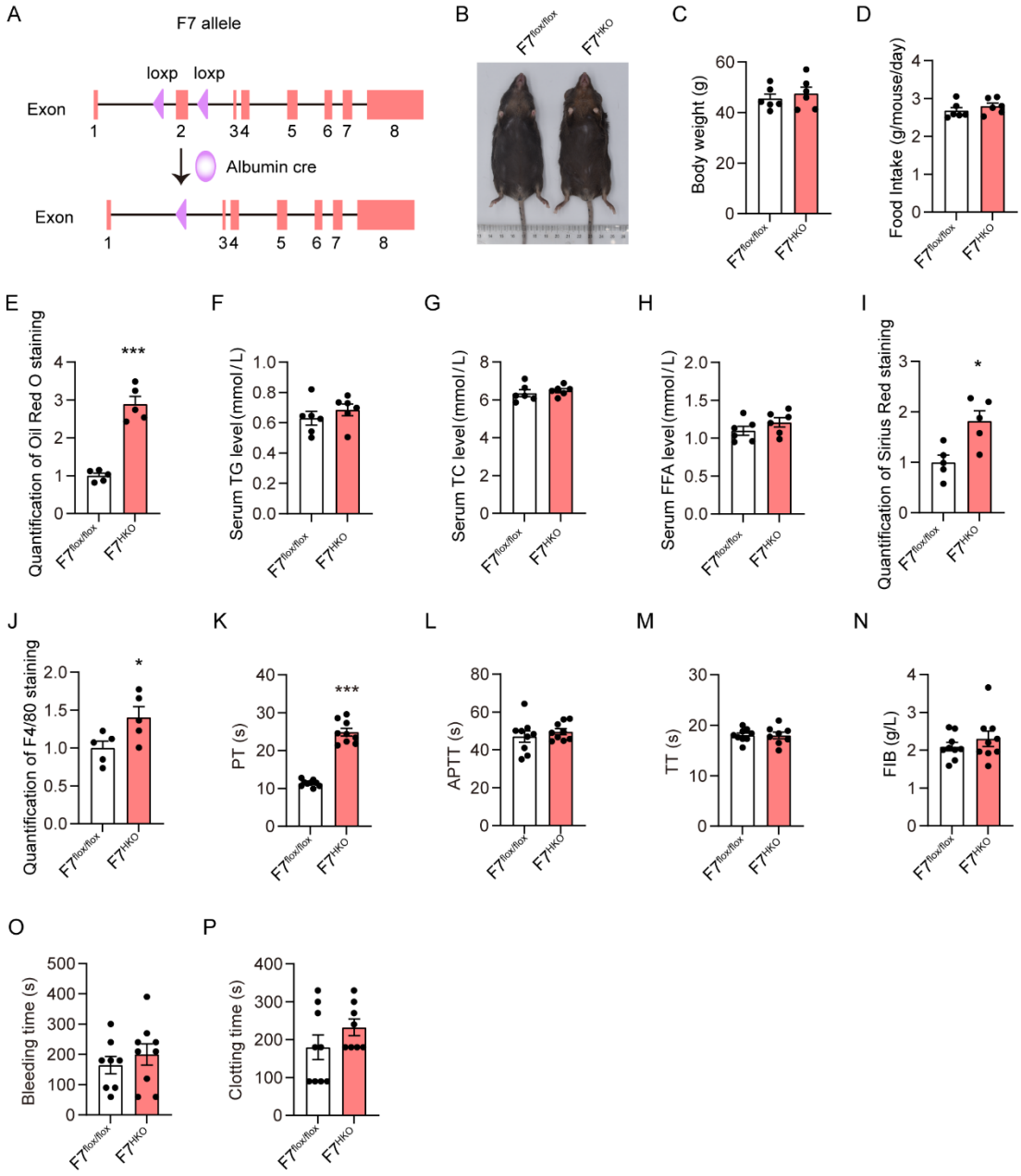

Figure S4. Evaluation of the metabolic parameters and coagulation homeostasis in hepatic specific F7 knockout mice, related to Figure 3

(A) Schematic diagram of $F7^{HKO}$ mice ($F7^{flox/flox}$, *Albumin*-cre mice) construction.

(B) The representative photograph of $F7^{flox/flox}$ and $F7^{HKO}$ mice.

(C) Body weight of $F7^{flox/flox}$ and $F7^{HKO}$ mice (n = 6 / group).

(D) Food intake of $F7^{flox/flox}$ and $F7^{HKO}$ mice (n = 6 / group).

(E) Quantitative analysis of Oil Red O staining from panel (F) in Figure 3.

(F) Serum TG levels of $F7^{flox/flox}$ and $F7^{HKO}$ mice (n = 6 / group).

(G) Serum TC levels of $F7^{flox/flox}$ and $F7^{HKO}$ mice (n = 6 / group).

(H) Serum FFA levels of $F7^{flox/flox}$ and $F7^{HKO}$ mice (n = 6 / group).

(I) Quantitative analysis of Sirius Red staining from panel (J) in Figure 3.

(J) Quantitative analysis of F4/80 staining from panel (J) in Figure 3.

(K) The prothrombin time (PT) of $F7^{flox/flox}$ and $F7^{HKO}$ mice (n = 9 / group).

(L) The activated partial thromboplastin time (APTT) of $F7^{flox/flox}$ and $F7^{HKO}$ mice (n = 9 / group).

(M) The thrombin time (TT) of $F7^{flox/flox}$ and $F7^{HKO}$ mice (n = 9 / group).

(N) The plasma fibrinogen (FIB) levels of $F7^{flox/flox}$ and $F7^{HKO}$ mice (n = 9 / group).

(O) The tail bleeding time of $F7^{flox/flox}$ and $F7^{HKO}$ mice (n = 9 / group).

(P) The blood clotting time of $F7^{flox/flox}$ and $F7^{HKO}$ mice (n = 9 / group).

Data are presented as mean ± S.E.M. Significance was assessed by Student's t test (C-O) or Mann-Whitney U test (P). * $P < 0.05$, *** $P < 0.001$ versus control.

Figure S5

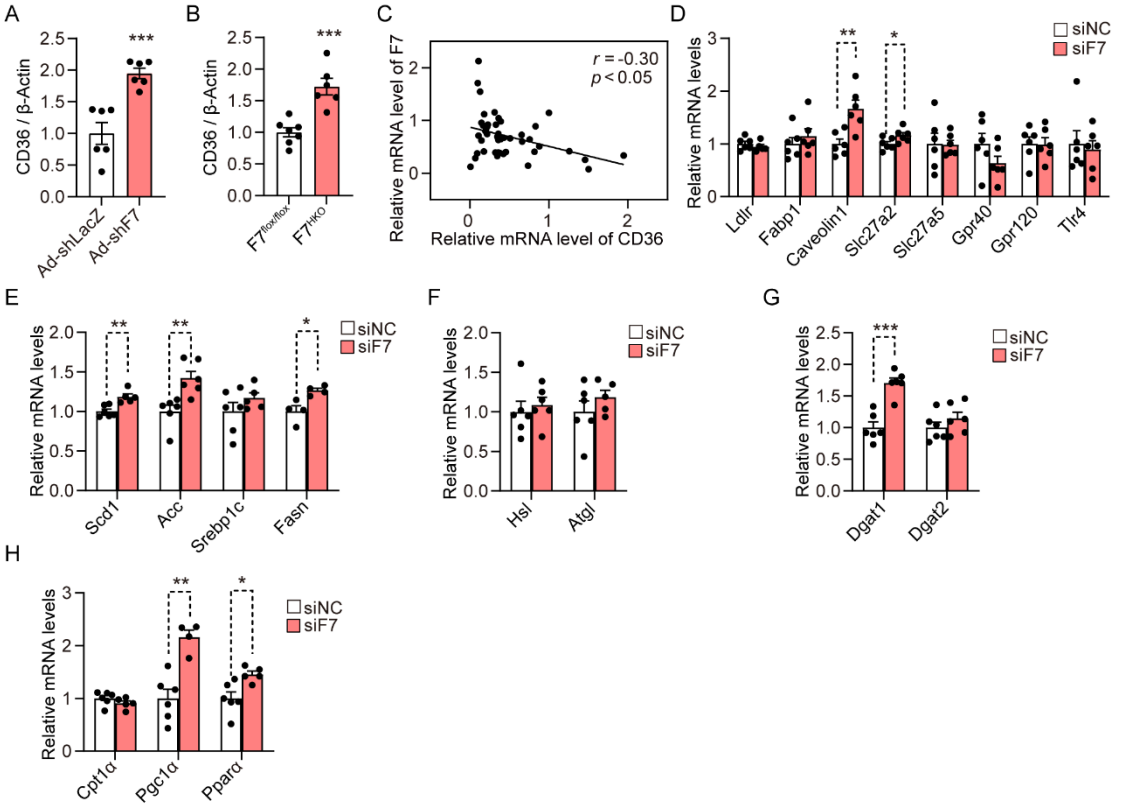

Figure S5. FVII exerts mild function in other lipid metabolic process, related to Figure 4

(A, B) Quantitative analysis of CD36 expression from panel (K) and (L) in Figure 4, respectively.

(C) Correlation analysis between hepatic *F7* and *Cd36* mRNA level in individuals with or without NAFLD (n = 45).

(D-H) RT-qPCR analysis of genes related to lipid transport (D), *de novo* lipogenesis (E), lipolysis (F), FA esterification (G), and β oxidation (H) in primary hepatocyte treated with FFA for 12 h after transfection with siNC or siF7 for 48 h.

Data are presented as mean ± S.E.M. Significance was assessed by Student's t test (A, B, D-H) or Spearman correlation (C). * $P < 0.05$, ** $P < 0.01$, *** $P < 0.001$ versus

control.

Figure S6

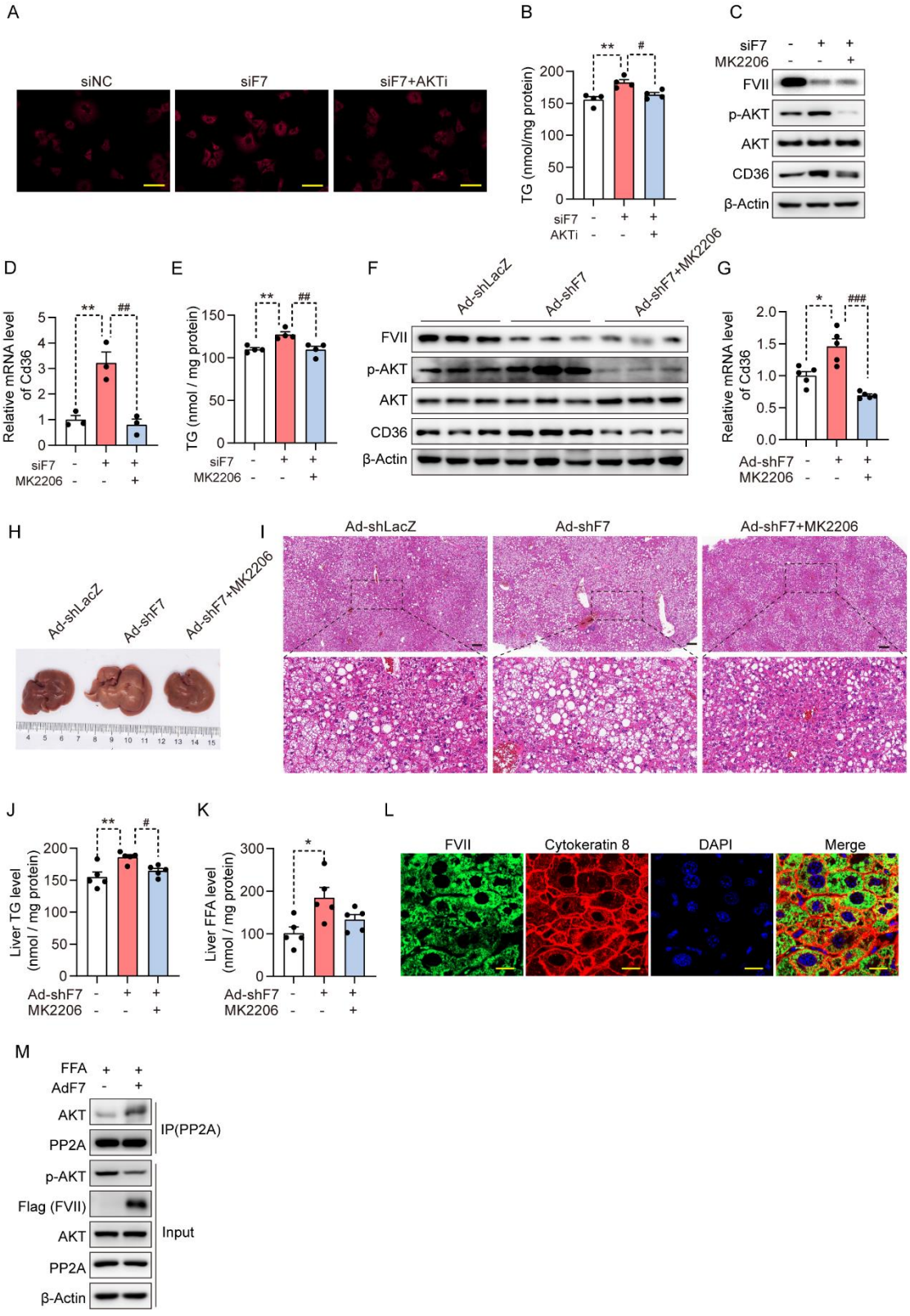

Figure S6. FVII modulates CD36 expression via activating AKT signaling, related to Figure 6.

(A) Representative Nile Red staining of primary hepatocytes transfected with siNC or siF7 for 24 h and in the absence or presence of AKTi (10 μM) for another 24 h. Scale bar, 100 μm.

(B) Cellular TG contents of primary hepatocytes transfected with siNC or siF7 in the absence or presence of AKTi (10 μM).

(C) Immunoblot analysis of indicated protein levels in primary hepatocytes transfected with siNC or siF7 for 48 h, in the presence or absence of MK2206 (1 μM). β-Actin was used as a loading control.

(D) RT-qPCR analysis of *Cd36* mRNA levels in primary hepatocytes transfected with siNC or siF7 for 48 h, in the presence or absence of MK2206 (1 μM).

(E) Cellular TG levels of primary hepatocytes transfected with siNC or siF7 for 48 h, in the presence or absence of MK2206 (1 μM).

(F) Immunoblot analysis of indicated protein levels in the livers of Ad-shLacZ, Ad-shF7 and MK2206-treated Ad-shF7 mice. β-Actin was used as a loading control.

(G) RT-qPCR analysis of *Cd36* mRNA levels in the livers of Ad-shLacZ, Ad-shF7 and MK2206-treated Ad-shF7 mice. $n = 5$ / group.

(H) Representative liver photographs of Ad-shLacZ, Ad-shF7 and MK2206-treated Ad-shF7 mice.

(I) Representative images of H&E staining from liver sections of Ad-shLacZ, Ad-shF7 and MK2206-treated Ad-shF7 mice. Scale bar, 200 μm.

(J) Liver TG levels of Ad-shLacZ, Ad-shF7 and MK2206-treated Ad-shF7 mice. $n = 5$ / group.

(K) Liver FFA levels of Ad-shLacZ, Ad-shF7 and MK2206-treated Ad-shF7 mice. $n = 5$ / group.

(L) Immunofluorescence staining of FVII (green), cytokeratin 8 (red) and DAPI (blue) in liver section of wildtype mice. Scale bar, 10 μm.

(M) Immunoblot analysis of the indicated protein levels enriched by immunoprecipitation of PP2A in FFA-treated Ad-ctrl and Ad-F7 primary hepatocytes. β-Actin was used as a loading control.

Data are presented as mean ± S.E.M. Significance was assessed by one way ANOVA (B, D, E, G, J, K). * or $^{\#}P < 0.05$, ** or $^{\#\#}P < 0.01$, $^{\#\#\#}P < 0.001$ versus control.

Figure S7

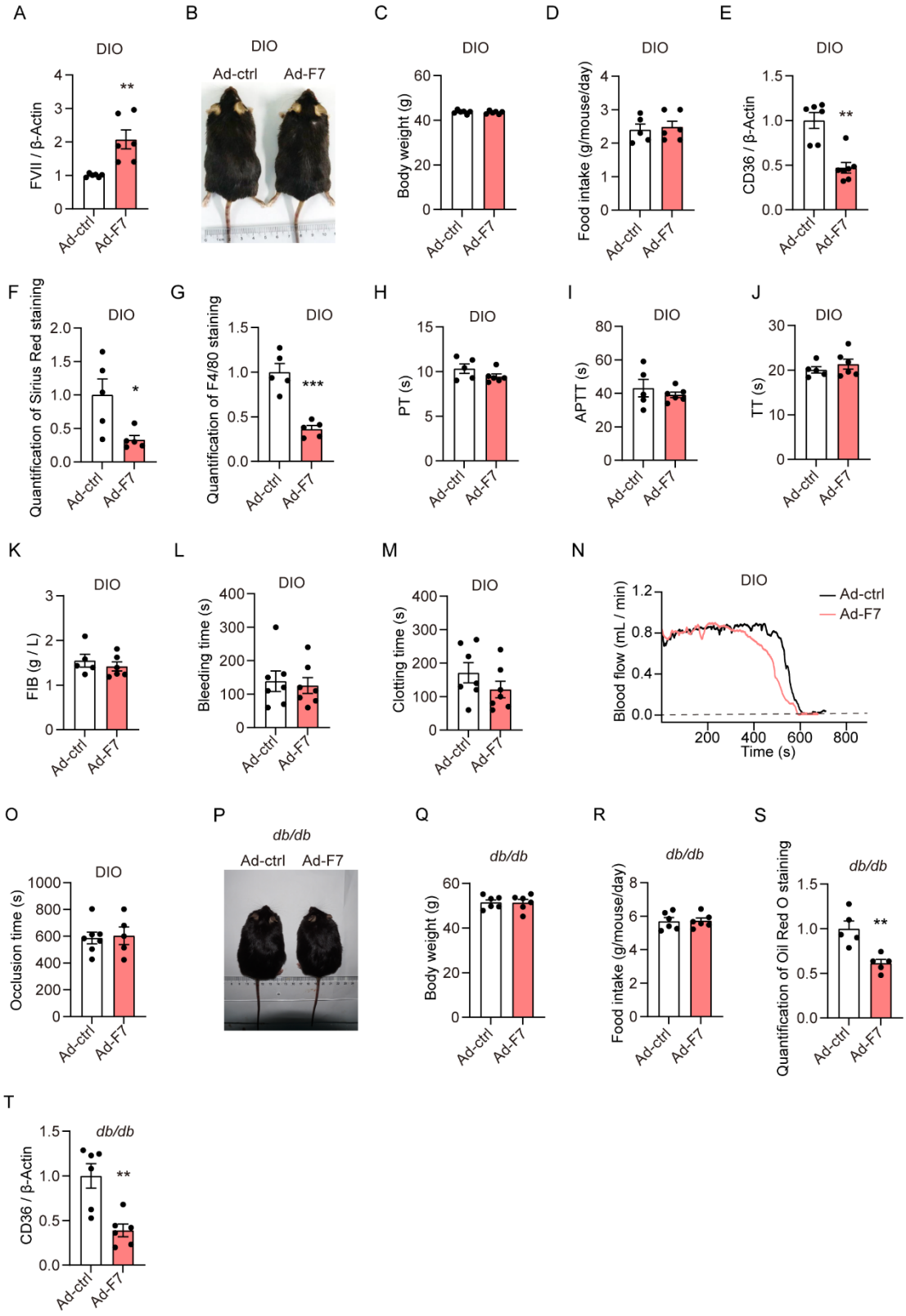

Figure S7. Overexpression of hepatic FVII does not alter coagulation homeostasis, related to Figure 7.

(A) Quantitative analysis of FVII protein abundance from panel (B) in Figure 7.

(B) The representative photograph of Ad-ctrl and Ad-F7 DIO mice.

(C) Body weight of Ad-ctrl and Ad-F7 DIO mice (*n* = 6 / group).

(D) Food intake of Ad-ctrl and Ad-F7 DIO mice (*n* = 5-6 / group).

(E) Quantitative analysis of CD36 protein abundance from panel (I) in Figure 7.

(F) Quantitative analysis of Sirius Red staining from panel (K) in Figure 7.

(G) Quantitative analysis of F4/80 staining from panel (K) in Figure 7.

(H) The prothrombin time (PT) of Ad-ctrl and Ad-F7 DIO mice (*n* = 5-6 / group).

(I) The activated partial thromboplastin time (APTT) of Ad-ctrl and Ad-F7 DIO mice (*n* = 5-6 / group).

(J) The thrombin time (TT) of Ad-ctrl and Ad-F7 DIO mice (*n* = 5-6 / group).

(K) The plasma fibrinogen (FIB) levels of Ad-ctrl and Ad-F7 DIO mice (*n* = 5-6 / group).

(L) The tail bleeding time of Ad-ctrl and Ad-F7 DIO mice (*n* = 7 / group).

(M) The blood clotting time of Ad-ctrl and Ad-F7 DIO mice (*n* = 7 / group).

(N) Blood flow records of $FeCl_3$-induced carotid artery thrombosis formation in Ad-ctrl and Ad-F7 DIO mice.

(O) The occlusion time of $FeCl_3$-treated carotid artery in Ad-ctrl and Ad-F7 DIO mice (*n* = 5-7 / group).

(P) The representative photograph of Ad-ctrl and Ad-F7 *db/db* mice.

(Q) Body weight of Ad-ctrl and Ad-F7 *db/db* mice (*n* = 6 / group).

(R) Food intake of Ad-ctrl and Ad-F7 *db/db* mice (*n* = 6 / group).

(S) Quantitative analysis of Oil Red O staining from panel (R) in Figure 7.

(T) Quantitative analysis of CD36 protein abundance from panel (Y) in Figure 7.

Data are presented as mean ± S.E.M. Significance was assessed by Student's *t* test (A, C, D, F-M, O, Q-T) or Mann-Whitney *U* test (E). * $P < 0.05$, ** $P < 0.01$, *** $P < 0.001$ versus control.

Table S1. Mice characterizations

NO.	Body weight (g)	Liver weight (g)	Liver TG level (nmol/mg protein)	Liver TC level (nmol/mg protein)	liver FFA level (nmol/mg protein)
1	54.5	2.88	290.41	18.13	339.51
2	53.2	3.56	304.81	18.88	357.76
3	56.3	3.47	317.55	20.55	425.02
4	51.7	2.63	323.24	20.75	522.95
5	56.2	3.4	324.11	19.97	561.16
6	54	3.48	343.75	22.02	575.13
7	47.7	2.45	308.95	18.68	523.49
8	58.5	2.91	295.10	17.90	340.90
9	52.7	3.18	322.26	18.38	517.26
10	49.8	2.36	271.72	15.64	352.60
11	45.5	1.3	233.81	14.43	382.16
12	38.2	1.29	227.99	14.07	404.88
13	47.5	1.47	240.37	14.75	412.58
14	55	3	291.65	18.51	456.25
15	60.1	3.6	301.07	19.29	474.90
16	55	3.25	326.05	20.12	514.42
17	48.4	1.84	271.44	16.76	406.83
18	46.7	2.15	256.55	15.76	404.03
19	39.4	1.04	269.06	17.42	465.29
20	51.7	2.42	268.73	15.87	404.73
21	49.6	2.98	300.07	17.11	364.24
22	43.8	1.29	291.48	16.56	435.16

Table S2: siRNA sequences and primer sequences list

siRNA sequences	
Genes (mouse)	**siRNA oligo**
F7	GCTTCTGCCTCCTAGACTT
CD36	CACAUACAGAGUUCGUUAU
Genes (human)	**siRNA oligo**
F7	GCCTCACAGAGTCTTCGTA
qRT-PCR primers	
Genes (mouse)	**Primer sequence**
18S	CGCCGCTAGAGGTGAAATTCT
	CATTCTTGGCAAATGCTTTCG
F7	AAAGGCGTGCCAACTCACTC
	CCTACGTTCTGACATGGATTCG
CD36	ATGGGCTGTGATCGGAACTG
	GTCTTCCCAATAAGCATGTCTCC
Hnf4α	AAGGTGCCAACCTCAATTCATC
	CACATTGTCGGCTAAACCTGC
F4/80	CCATCCACTTCCAAGATGGGTTA
	TGCCATCAACTCATGATACCCT
IL1b	TGCCACCTTTTGACAGTGATG
	TGATGTGCTGCTGCGAGATT
IL6	CTGCAAGAGACTTCCATCCAG
	AGTGGTATAGACAGGTCTGTTGG
Fibronectin	GCTCAGCAAATCGTGCAGC
	CTAGGTAGGTCCGTTCCCACT
Tgfb	CTTCAATACGTCAGACATTCGGG
	GTAACGCCAGGAATTGTTGCTA
Ire1α	ACACCGACCACCGTATCTCA
	CTCAGGATAATGGTAGCCATGTC
Chop	CTGGAAGCCTGGTATGAGGAT
	CAGGGTCAAGAGTAGTGAAGGT
Xbp1s	CTGAGTCCGAATCAGGTGCAG
	CCATGGGAAGATGTTCTGG

Perk	AGTCCCTGCTCGAATCTTCCT
	TCCCAAGGCAGAACAGATATACC
Atf6	GACTCACCCATCCGAGTTGTG
	CTCCCAGTCTTCATCTGGTCC
Ldlr	TGACTCAGACGAACAAGGCTG
	ATCTAGGCAATCTCGGTCTCC
Pgc1α	CCCTGCCATTGTTAA GACC
	TGCTGCTGTTCCTGTTTTC
PPARα	GCGTACGGCAATGGCTTTAT
	GAACGGCTTCCTCAGGTTCTT
Srebp1c	GGAGCCATGGATTGCACATT
	GGCCCGGGAAGTCACTGT
Acc	TGACAGACTGATCGCAGAGAAAG
	TGGAGAGCCCCACACACA
Fasn	GCTGCGGAAACTTCAGGAAAT
	AGAGACGTGTCACTCCTGGACTT
Scd1	TCCCTCCGGAAATGAACGAGAGAA
	AGTGCAGCAGGACCATGAGAATGA
Cpt1α	TTCACTGTGACCCCAGACGGG
	AATGGACCAGCCCCATGGAGA
Hsl	TCAAGCCAAGGTGTCCTCCACATG
	GGGTGCAAGAGGTCTTTTAGTGCC
Atgl	GGATGGCGGCATTTCAGACA
	CAAAGGGTTGGGTTGGTTCAG
Slc27a2	TCCTCCAAGATGTGCGGTACT
	TAGGTGAGCGTCTCGTCTCG
Slc27a5	CTACGCTGGCTGCATATAGATG
	CCACAAAGGTCTCTGGAGGAT
Tnfα	CCCTCACACTCAGATCATCTTCT
	GCTACGACGTGGGCTACAG
Ccl2	TTAAAAACCTGGATCGGAACCAA
	GCATTAGCTTCAGATTTACGGGT
CD68	TGTCTGATCTTGCTAGGACCG
	GAGAGTAACGGCCTTTTTGTGA

Col1a1	GCTCCTCTTAGGGGCCACT
	CCACGTCTCACCATTGGGG
Col3a1	CTGTAACATGGAAACTGGGGAAA
	CCATAGCTGAACTGAAAACCACC
Ctgf	GGGCCTCTTCTGCGATTTC
	ATCCAGGCAAGTGCATTGGTA
Timp1	GCAACTCGGACCTGGTCATAA
	CGGCCCGTGATGAGAAACT
Dgat1	TCCGTCCAGGGTGGTAGTG
	TGAACAAAGAATCTTGCAGACGA
Dgat2	GCGCTACTTCCGAGACTACTT
	GGGCCTTATGCCAGGAAACT
qRT-PCR primers	
Genes (human)	**Primer sequence**
18S	TTCGAACGTCTGCCCTATCAA
	ATGGTAGGCACGGCGACTA
F7	CGGACGTTCTCTGAGAGGAC
	GGCACGTTGAGGACCATGAG
HNF4α	CGAAGGTCAAGCTATGAGGACA
	ATCTGCGATGCTGGCAATCT
CD36	GGCTGTGACCGGAACTGTG
	AGGTCTCCAACTGGCATTAGAA
Primer sequences for plasmid construction	
pLVX-F7(mouse)-Flag	CCGCTCGAGATGGTTCCACAGGCGCATGGGCT
	CCGGAATTCCTACTTGTCGTCGTCGTCCTTGTAGTCCAGTAGTGGGAGTCGGAAAAC
pLVX-F7(human)-Flag	CCGCTCGAGATGGTCTCCCAGGCCCTCAGGCTC
	CCGGAATTCCTACTTGTCGTCGTCGTCCTTGTAGTCGGGAAATGGGGCTCGCAGGAG
Adv-F7-Flag	CACCATGGTTCCACAGGCGCATG
	CTACTTGTCGTCGTCGTCCTT
Adv-F7 mut-Flag	CACCATGGTTTTCATAACCCAGGAGG
	CTACTTGTCGTCGTCGTCCTT

Adv-F7-shRNA	CACCGCTTCGATAATATCCGCTACTCGAAAGTAGCGGA TATTATCGAA GC